General Disclaimer

One or more of the Following Statements may affect this Document

- This document has been reproduced from the best copy furnished by the organizational source. It is being released in the interest of making available as much information as possible.

- This document may contain data, which exceeds the sheet parameters. It was furnished in this condition by the organizational source and is the best copy available.

- This document may contain tone-on-tone or color graphs, charts and/or pictures, which have been reproduced in black and white.

- This document is paginated as submitted by the original source.

- Portions of this document are not fully legible due to the historical nature of some of the material. However, it is the best reproduction available from the original submission.

(NASA-TM-79023) SOME HEAT TRANSFER AND HYDRODYNAMIC PROBLEMS ASSOCIATED WITH SUPERCONDUCTING CABLES (SPTL) (NASA) 28 p
HC A03/MF A01 CSCL 20D

N79-15267

Unclas
G3/34 43373

DOE/NASA/0207-78/1
NASA TM-79023

SOME HEAT TRANSFER AND HYDRODYNAMIC PROBLEMS ASSOCIATED WITH SUPERCONDUCTING CABLES (СПК - SPTL)

Robert C. Hendricks
National Aeronautics and Space Administration
Lewis Research Center

David E. Daney
National Bureau of Standards

and

V. M. Yeroshenko, Ye. V. Kuznetsov, and O. A. Shevchenko
G. M. Krzhizhanovsky Power Institute (ENIN)

Work performed for
U. S. DEPARTMENT OF ENERGY
Office of Energy Technology
Division of Electric Energy Systems

TECHNICAL PAPER
U.S. - U.S.S.R. Committee for Superconducting Power Transmission
Upton, Long Island, New York, October 5-6, 1978

SOME HEAT-TRANSFER AND HYDRODYNAMIC PROBLEMS ASSOCIATED WITH SUPERCONDUCTING CABLES (СПК-SPTL)

by Robert C. Hendricks
National Aeronautics and Space Administration
Lewis Research Center
Cleveland, Ohio 44135

David E. Daney
National Bureau of Standards
Bolder, Colorado 30302

and

V. M. Yeroshenko, Ye. V. Kuznetsov,
and O. A. Shevchenko
G. M. Krzhizhanovsky Power Institute (ENIN)
Moscow, U.S.S.R.

INTRODUCTION

As СПК-SPTL technology advances, one must become more concerned with heat input to the coolant from the cable, the dielectric materials, and heat leaks and how these heat sources affect system hydrodynamics, including the refrigerator. While scaled model facilities have operated successfully, no completely coupled system has functioned, and many questions in heat transfer and hydrodynamics remain unanswered.

Similary, one must be concerned with the economics. One may recall that several years ago conventional cable technology was limited to 1/2 to 3/4 GW. With planned power complexes of 1 to 2 GW, the economic advantage of СПК-SPTL was clear; however, the reality of СПК-SPTL advances stimulated the development of conventional cables and now the economics are unclear. The danger of economics pacing science is that breakthroughs are not favored as they are unknown, while current practice dominates; such practices can spawn economic demise.

E-9820

With these thoughts in mind, we will present some results of an experiment conducted at ENIN in a heated, horizontal tube using fluid helium as the coolant; discuss some stability problems of the coupled, liquifier-heated tube system; and propose some future experiments. The basic data and description of the apparatus may be found in the Protocol Record[1] (ref. 1, appendix 3).

APPARATUS

The experimental apparatus (fig. 1), consisted of a (1) liquifier, (2) a transfer line, (3) service access can, (4) flow control and diverter, (5) the horizontal test section, (6) a gasifier, (7) flow measurement, (8) gas holder, and (9) nitrogen supply. The system could be operated in the open or closed mode. The apparatus was 3 m long with a 2.85-m heated test section, 1.9 cm φ, see figure 2. An interval probe 0.6 cm φ with two thermocoupled rakes was positioned to give interval temperature distributions, see figure 3. Data from these rakes are not yet available.

The Thermocouples* were placed at the top (0 position) and bottom (π position) of the horizontal test section with thermocouples placed around the circumference at X/L = 0.57. The instrumentation positions given on figure 4 are tabulated below:

---

[1]The visit included the Krzhizhanovsky Energy Institute, Moscow; the Luikov Heat and Mass Transfer Institute of the Academy of sciences, Belorussia Minsk; the Thermophysics Institute - Siberian Branch of the Academy of Sciences U.S.S.R., Novosibirsk; and the Kurchatov Institute of Atomic Energy Moscow. The Protocol contains 13 appendixes which relate the joint studies undertaken while in the Soviet Union.

*0.1% Fe + 0.1% Zn ÷ Cu vs Cu with ice reference.

Position	Length, m	(X/L)
1	0.415	0.146
2	0.740	.26
3	1.07	.375
4	1.625	.57
5	2.165	.759
6	2.320	.814
7	2.850	1

A more detailed description can be found in the Protocol Record of our visit (ref. 1).

RESULTS AND DISCUSSION

Six experimental data points were taken. The range of control parameters are as follows:

Pressure	1.2-3.0 atm
Inlet temperature	6.5-15.0 K
Heat input	28.7-210.0 W
	0.0169-0.124 mW/cm^2
Mass flow	0.52-4.7 g/s
	0.2-1.84 g/cm^2-sec

$A_{x_c} = 2.55\ cm^2$; $As = 1700\ cm^2$; $d_H = 1.3$ cm

The data points are tabulated in reference 1, and reproduced in part as table I. The experimental parameters of table I are followed by several conventional parameters: Reynolds, Prandtl, Grashoff, and reduced Nusselt numbers along with the ψ or ψ^* parameter used by several authors to correlate heat transfer data (e.g. Kutateladze (ref. 2), Yaskin, et. al. (refs. 3 and 5), and Hendricks (refs. 4 and 5). These parameters will be used in subsequent discussions of the data.

The variation of wall temperature with circumferential position at X/L = 0.52 is presented in dimensionless form as figure 5. The profiles are rather conventional except for runs 6 and 10, where substantially higher temperatures near the top of the tube are noted. The variation of temperature from top to bottom was up to 6.5 K, a considerable effect when one considers the bulk temperature near 10 K.

Typical axial temperature profiles are shown as figure 6, where the bulk temperature is calculated - not measured. The large drop in wall temperature at X/L = 0.814 may be due to the presence of the internal bulk temperature probe, or end effects, see figure 4.† The general trends are characteristic of heated tube data for near critical fluids, i.e. an abrupt rise in temperature followed by a decrease to some point where the profile again increases.

The separation of the profiles from $\theta = 0$ to $\theta = \pi$ is characteristic of near critical data from curved tubes, where the body force can be thought of as the imposed force ($V^2/R = ng$).

Attempts to correlate the data using the reduced Nusselt (Nu/Nu_c) and Grashoff (Gr/Gr_L) numbers was unsuccessful. Similarly attempts to correlate these data as functions of Gr, Re, Nu groups did not prove of value.

Realizing that the profiles were similar to those of other near critical data and the success of correlations similar to those proposed by (Yaskin et. al. (refs. 3 and 5) and Hendricks (refs. 4 and 5)), these same parameters were applied to the data. Figure 7(a) presents data for the lower surface, $\theta = \pi$,‡ There appears to be a rapid deterioration in heat transfer as the ψ or ψ^* parameter increases, over that which would be expected if a gas or liquid at low ΔT were flowing through the tube in the absence of Grashoff effects. The lower limit, at high values of ψ must eventually approach that of the tube at high Reynolds numbers; however, these data do not cover this range. Figure 7(b) presents data for the upper surface, $\theta = 0$. Again there is a deterioration, however it is not as strong with increasing ψ or ψ^* except near $\psi = 1$. While these groupings are preliminary, they do agree with other near critical results and may prove useful in correlating thermogravitational data.

---

†The reasons for $T_{w_\pi} < T_b$, runs 14 and 16 are unknown.

‡Run 16 was not stable, W ~ 1 g/s.

The average results were obtained by considering the temperature profiles of figure 5. Defining $y = 1/\pi \int (T_w - T_\pi / T_0 - T_\pi) d\theta = 1/\pi \int \varphi \, d\theta$ and evaluating the Nusselt and ψ parameters as:

$$\overline{Nu}_R = y \, Nu_{R0} + (1 - y) Nu_{R\pi}$$

$$\overline{\psi} = y \, \psi_0 + (1 - y) \psi_\pi$$

Figure 7(c) was constructed. It is interesting to note that the data scatter about ±20 percent for figures 7(a) to (c).

Now the value of Nu_R must be modified to consider Grashoff effects at very low values of Reynolds number, however, the present groupings appear useful and tie quite well with the work of reference 1, appendices 8 and 9, and that of Hendricks. The theoretical analysis should be developed from these appendices as a starting point.

The numerical calculations of Skiadaressis and Spalding of reference 6 in predicting the experimental results of Petukhov et. al. reference 7 is impressive. While the theoretical approach differs from that of reference 1 it must be considered as viable, but near critical (real) fluid property concepts need to be integrated into the analysis.

The set of figures 8(a) to (d) serve to illustrate changes in thermogravitational effects at various values of (X/L). Data for $X/L = 0.814$ appear to be end effects or affected by the probe; however, this remains to be proven. While these data are indeed functions of (X/L), we tried to determine how the data for $0.26 \leq (X/L) \leq 0.759$ would group if (X/L) effects were ignored and all data were placed on the same plot, see figure 9. Here the average values of reduced Nusselt number are presented as a function of ψ (or ψ^*) and the dashed lines represent bounds of ±20 percent. Four points at $X/L = 0.759$ are beyond these bounds; two are at 30 percent and two runs 14 and 16 are significantly beyond, recall figure 4.

Some further discussion is presented in Appendix A.

REFRIGERATOR/LIQUIFIER OSCILLATIONS

During the cool down, it was difficult to achieve operating conditions; however a more serious problem developed in the course of the experiment. The system began to oscillate at 1-2 cycles/minute at inlet temperatures near 6.5 K for pressures of 2 to 3.5 atm. The temperature and pressure perturbations were in phase as reported by Daney and fed through to the liquifier. The flow perturbation was out of phase; however, a considerable line length with a gasifier is probably responsible.

A typical oscillation growth pattern is given as figure 10(a). The steady oscillation shown as figure 10(b) has a multiplicity of harmonics. The pressure (temperature) wave is illustrated as figure 10(c).

While these profiles are undocumented their presence requires further investigation. Unfortunately such experiments can not be continued by Daney and will require transient type recording equipment at ENIN. The instabilities should be separated from those self induced through manual control of the ENIN System.

PROPOSED WORK

Continuation of this experiment at ENIN will certainly clarify many of the existing problems however we should like to propose some tests and cite some problems in addition to those cited in reference 1, appendix 3.

1. Adiabatic flow of helium at three pressures and flow rates to evaluate system thermometry and heat leakage.

2. Decrease the heat input to the order of tenths mW/cm^2 (and less). The experimental data of this paper attempted to demonstrate thermogravitational effects and found them significant at these heat fluxes (to 0.12 W/cm^2). While the boiling flux is ~1 W/cm^2, line losses are anticipated to be as low as 0.1 to 0.01 mW/cm^2.

3. Stratification effects in very long lines remain unanswered. Low heat capacity and conductivity along with slow moving cellular patterns could lead to stratified flows. For a solid tubular CIIK-SPTL the result would be a resistive region near the top of the cable. In this case the current would shift to the lower surface but a portion of the cable would func-

tion at reduced capacity. The power transport would be degraded. For twisted strands, the strands would be alternately in and out of the region raising the overall resistance of the cable. This also degrades power transmission.

4. Fault Propagation/Recovery must be assessed in view of the propagation of heat pulses in a long line. Daney has demonstrated that in the adiabatic case the perturbation traverses the tube unimpeded, while under heating the disturbance grows. If the power is dropped after a fault, until the section recovers, the heat pulse is still traveling along with the flow. Subsequent start up without considering such a pulse will simply revert to another heat pulse in the system (perhaps 2n where n = number of starts if the original point were not fully recovered at each start).

5. Some systems have indicated that separation of the flow streams is necessary; it may however be due to the thermal stratification cited in 4 or to the usual central thermal hump in diabatic counterflow heat exchangers. Nevertheless some cable manufactures have proposed separate go and return tubes, but economics as well as thermal analyses of these proposals is necessary.

6. Test of coaxial heated tubes simulating cables need to be conducted. While figures 11(a) to (d) are for laminar convection of air without forced flow, the secondary circulation in forced flows have similar characteristics. As can be seen the central tube can afford a major temperature gradient from the bottom to the top when thermogravitational effects are important - such as in near critical fluids. For $D_o/D_i = 1.3$ and large ΔU, the system remains nearly axisymmetric and buoyancy has little effect (fig. 11(a)). At $D_o/D_i = 1.95$, at smaller ΔU, buoyancy becomes significant (fig. 11(b)). At $D_o/D_i = 3.9$ and 4.9, the effects are pronounced and at large ΔU, the effects are severe (figs. 11(c) and (d). (figs. 11(a) to (d) courtesy of Prof. U. Grigill, Tech. Univ. of Munich - FRG)

ACKNOWLEDGEMENT

The assistance of John Hendricks in the preparation of this paper is acknowledged.

SYMBOLS

D	diameter, cm
d_H	hydraulic diameter, cm
Gr	Grashoff number-modified, $g\beta q\, d_H^4/\lambda\eta^2$
Gr_L	Limiting Grashoff number, $3.0\times10^{-5}\, Re^{11/14} Pr^{1/2} \times [1 + 2.4(Pr^{2/3} - 1)Re^{-1/8}]$
g	acceleration of gravity, cm/sec^2
H	enthalpy, j/gm
ΔH	enthalpy difference, j/gm, $H_w - H_B$
L	test section length, cm
Nu	Nusselt number, $\alpha\, d_H/\lambda$
Nu_R	Reduced Nusselt number, Nu_{exp}/Nu_{calc}
n	integer
P	pressure, MPa
Pr	Prandtl number
Q	heat input, W
q	heat flux, W/cm^2
R	radius of curvature, cm
Re	Reynolds number
T	temperature, K
ΔT	temperature difference, K, also ΔU, $(T_w - T_B)$
V	velocity, cm/sec
W	mass flow rate, gm/sec
x	axial position, cm
y	average temperature fraction, $1/\pi \int \varphi\, d\theta$

α heat transfer coefficient, $W/cm^2\text{-}K$ ($W/m^2\text{-}K$ in tables)

β volumetric expansion coefficient, K^{-1}, $-\partial \ln\rho/\partial T$

θ circumferential position

φ dimensionless temperature parameter, $(T_w - T_\pi)/(T_0 - T_\pi)$

ψ $1 + \beta\Delta T$

ψ^* $1 + (\partial \ln\rho/\partial H)\ \Delta H$

τ time

Subscripts:

B evaluated at bulk

calc calculated

exp experimental

i inside

in inlet

o outside

w evaluated at wall

0 evaluated at $\theta = 0$

π evaluated at $\theta = \pi$

APPENDIX A

With only limited data and analytical backup, detailed analysis of the results is unwarranted. However some useful observations can be made. For fluid helium in its near-critical thermodynamic state in forced flow through a uniformly heated horizontal tube:

(a) For heat fluxes less than 100 mW/cm^2 the secondary flows or thermogravitational effects are significant and cause thermal stratification to 6 K with a bulk temperature of 10 K.

(b) The power law dependency of ψ and Nu_R of figure 11, where $\overline{Nu}_R \sim \overline{\psi}^{-n}$ for $4/5 \leq n \leq 5/4$ is stronger than for vertical flow in tubes where $n \sim 1/2$. This indicates a more rapid deterioration in heat transfer than for the vertical tube with increases in ψ or ψ^*.

(c) The use of $\overline{Nu}_R \sim 4/5\, \overline{\psi}^{-4/5}$ produces a reasonable prediction of temperature difference figure A1 and heat flux figure A2 but the issues at high values of ψ and for $\psi \rightarrow 1$ are not understood.

(d) The use of reduced Nusselt number (Nu_R) and the ψ or ψ^* parameters tend to group the data at high Reynolds numbers. However the effect of Grashoff number and buoyancy fluctuations will need to be added to these parameters respectively before the theory and correlations can be meaningful. This is of course true for both the horizontal and vertical orientation where up and down flows are common. Further, inclusion of two-dimensional effects in the theory to handle secondary flows seems necessary.

REFERENCES

1. PROTOCOL of the visit of American Experts on Hydrodynamics and Heat Transfer in Superconducting Transmission Lines. Moscow, USSR, Sept. 4-22, 1978.

2. Kutateladze, S. S. (Scripta Technics, Inc., transl.): Fundamentals of Heat Transfer. R. D. Cess, ed., Second Rev. and Augm. ed., Academic Press, 1963.

3. Yaskin, L. A.; et. al.: A Correlation of Heat Transfer to Supercritical Helium in Turbulent Flow in Small Channels. Cryogenics, Oct. 1977.

4. Hendricks, R. C.: Simulation of the Heat Transfer Characteristics of Lox. ASME Paper 77-HT-9, Aug. 1977.

5. Yaskin, L. A.; and Hendricks, R. C.: Private Communication and work under US-USSR Protocol Agreement, Ref. 1.

6. Skiadaressis, D.; and Spalding, D. B.: Prediction of Combined Free and Forced Convection in Turbulent Flow Through Horizontal Tubes. Lett. Heat Mass Transfer, vol. 4, no. 1, Jan.-Feb. 1977, pp. 35-40.

7. Petukhov, B. S.; et. al.: Turbulent Flow and Heat Transfer in Horizontal Tubes with Substantial Influence of Thermogravitational Forces. 5th International Heat Transfer, 1974, Vol. 3. Japan Society of Mechanical Engineers, Society of Chemical Engineers, 1974, pp. 164-168.

TABLE I. - EXPERIMENTAL AND CALCULATED PARAMETERS FOR NEAR CRITICAL FLUID HELIUM FLOWING THROUGH A UNIFORMLY HEATED HORIZONTAL PIPE

Run No. 2

	P, MPa	Q, W	W, g/s	T_{in}, K	$y = \frac{1}{\pi}\int \varphi \, d\theta$		
	0.1216	28.7000	0.5200	15.9000	0.45		
X/L	0.146	0.26	0.375	0.57	0.759	0.814	1
Tw_0	24.2000	25.3500	26.2500	28.0000	31.7000	25.0000	
Tw_π	22.7500	22.8000	23.1000	25.0000	26.6500	24.5000	
T_B	16.5200	17.7100	18.9200	20.9700	22.9700	22.5510	25.5100
α_0	22.0000	22.1000	23.0000	25.0000	19.3400	113.3000	
α_π	27.1000	33.2000	40.3800	41.9000	45.8600	177.7000	
$T\theta$	28.0000	28.1500	26.4000	24.9000	25.0000		
Re	.835+04	.799+04	.765+04	.716+04	.676+04	.684+04	
Pr	.683	.687	.691	.695	.696	.696	
Gr	.153+09	.108+09	.779+08	.469+08	.299+08	.328+08	
Gr_L	.125+07	.111+07	.989+06	.828+06	.706+06	.729+06	
Nu_R $\theta = \pi$	.529	.646	.783	.807	.875	3.40	
Nu_R $\theta = 0$	.429	.430	.446	.462	.369	2.17	
Nu_R Avg.	.484	.549	.631	.652	.648	2.84	
ψ or ψ^* $\theta = 0$	1.48	1.44	1.40	1.34	1.39	1.07	
ψ or ψ^* $\theta = \pi$	1.39	1.29	1.23	1.20	1.16	1.04	
ψ or ψ^* Avg.	1.43	1.36	1.30	1.26	1.26	1.05	

Run No. 6

	P, MPa	Q, W	W, g/s	T_{in}, K	$y = \frac{1}{\pi}\int \varphi \, d\theta$		
	0.2047	67.7000	1.8400	10.3500	0.7		
X/L	0.146	0.26	0.375	0.57	0.759	0.814	1
Tw_0	17.8000	19.0000	19.2500	21.9000	22.0000	19.0000	
Tw_π	15.7000	15.4000	16.2500	17.3000	17.2500	17.5000	
T_B	11.3500	12.1200	12.9000	14.2600	15.6000	16.0000	17.2500
α_0	61.7000	68.5600	62.7000	52.1200	62.2000	131.0000	
α_π	91.5000	124.4300	118.8000	131.0000	241.3000	265.0000	
$T\theta$	21.9000	22.0000	21.3000	19.6000	17.3000		
Re	.370+05	.355+05	.341+05	.320+05	.303+05	.298+05	
Pr	699	.696	.694	.693	.693	.694	
Gr	.713+10	.502+10	.361+10	.215+10	.136+10	.119+10	
Gr_L	.790+08	.701+08	.627+08	.525+08	.450+08	.430+08	
Nu_R $\theta = \pi$	.656	.889	.848	.931	1.71	1.87	
Nu_R $\theta = 0$	.442	.490	.448	.371	.441	.927	
Nu_R Avg.	.506	.610	.568	.539	.821	1.21	
ψ or ψ^* $\theta = 0$	1.65	1.53	1.54	1.58	1.44	1.20	
ψ or ψ^* $\theta = \pi$	1.44	1.29	1.29	1.23	1.11	1.10	
ψ or ψ^* Avg.	1.58	1.46	1.46	1.47	1.34	1.17	

TABLE I. - Continued.

Run No. 10

		P, MPa	Q, W	W, g/s	T_{in}, K	$y = \frac{1}{\pi}\int \varphi \, d\theta$		
		0.3040	210.0000	4.7000	7.0000	0.75		
X/L		0.146	0.26	0.375	0.57	0.759	0.814	1
T_{w_0}		18.6000	19.4000	20.0000	23.4000	26.7500	21.3500	
T_{w_π}		16.2500	15.4500	15.9000	16.9000	17.8000	16.3000	
T_B		7.9000	8.6600	9.2000	11.0000	12.5000	12.9500	14.6500
α_0		115.0000	115.0000	114.0000	99.6000	86.7000	147.0000	
α_π		148.0000	182.0000	184.0000	209.0000	233.0000	368.0000	
$T\theta$		23.4000	24.2000	22.2000	20.6250	16.9000		
Re		.113+06	.107+06	.103+06	.936+05	.868+05	.850+05	
Pr		.827	.786	.766	.731	.717	.715	
Gr		.450+12	.245+12	.168+12	.594+11	.295+11	.244+11	
Gr_L		.194+10	.164+10	.147+10	.107+10	.857+09	.806+09	
Nu_R	$\theta = \pi$	.476	.595	.606	.696	.776	1.23	
	$\theta = 0$	.370	.376	.375	.332	.289	.490	
	Avg.	.396	.431	.433	.423	.411	.674	
ψ or ψ^*	$\theta = 0$	3.18	2.79	2.61	2.38	2.32	1.74	
	$\theta = \pi$	2.70	2.13	2.00	1.66	1.49	1.30	
	Avg.	3.06	2.63	2.46	2.20	2.11	1.63	

Run No. 14

		P, MPa	Q, W	W, g/s	T_{in}, K	$y = \frac{1}{\pi}\int \varphi \, d\theta$		
		0.1824	65.3000	1.08	6.5000	0.55		
X/L		0.146	0.26	0.375	0.57	0.759	0.814	1
T_{w_0}		21.4000	22.6000	22.1000	22.2000	22.8000	21.5000	
T_{w_π}		20.1000	20.4000	19.4000	18.4000	17.5000	14.3000	
T_B		8.13	9.26	10.45	12.54	14.62	15.23	17.31
α_0		28.95	28.79	32.97	39.76	46.96	61.3	
α_π		32.09	34.48	42.92	65.55	133.4	-------	
$T\theta$		22.2	22.	19.9	18.9	18.4		
Re		.270+05	.249+05	.230+05	.205+05	.186+05	.181+05	
Pr		.729	.708	.697	.690	.689	.690	
Gr		.359+11	.167+11	.850+10	.320+10	.145+10	.118+10	
Gr_L		.343+08	.266+08	212+08	.152+08	.116+08	.108+08	
Nu_R	$\theta = \pi$	.354	.381	.474	.719	1.45	-------	
	$\theta = 0$	.320	.318	.364	.436	.512	.666	
	Avg.	.335	.346	.413	.563	.936	-------	
ψ or ψ^*	$\theta = 0$	3.11	2.74	2.28	1.84	1.60	1.44	
	$\theta = \pi$	2.91	2.45	1.98	1.51	1.21	.935	
	Avg.	3.02	2.61	2.15	1.69	1.42	1.21	

TABLE I. - Concluded.

Run No. 15

	P, MPa	Q, W	W, g/s	T_{in}, K	$y = \frac{1}{\pi}\int \varphi \, d\theta$		
	0.2533	66.3000	1.0800	6.8000	0.55		
X/L	0.146	0.26	0.375	0.57	0.759	0.814	1
Tw_0	25.4000	23.6000	22.5000	22.5000	23.1000	22.2000	
Tw_π	22.3000	21.4000	19.7000	18.8000	18.7000	16.7000	
T_B	8.2000	9.3000	10.6000	12.7000	14.7000	15.9000	17.4000
α_0	22.7000	22.2700	32.7700	39.7900	46.4200	61.9000	
α_π	27.6600	32.3300	42.8500	63.9300	97.5000	487.5000	
$T\theta$	22.5	22.5	20.2	21.6	18.8		
Re	.259+05	.241+05	.223+05	.200+05	.183+05	.174+05	
Pr	.774	.740	.720	.705	.701	.700	
Gr	.726+11	.335+11	.158+11	.591+10	.276+10	.184+10	
Gr_L	.323+08	.254+08	.200+08	.145+08	.112+08	.981+07	
Nu_R $\theta = \pi$	.297	.351	.467	.695	1.06	5.27	
Nu_R $\theta = 0$	.244	.242	.357	.433	.503	.669	
Nu_R Avg.	.268	.291	.406	.551	.752	2.74	
ψ or ψ^* $\theta = 0$	3.99	3.43	2.35	1.87	1.62	1.42	
ψ or ψ^* $\theta = \pi$	3.45	2.67	2.03	1.54	1.30	1.05	
ψ or ψ^* Avg.	3.74	3.09	2.21	1.72	1.47	1.26	

Run No. 16

	P, MPa	Q, W	W†, g/s	T_{in}, K	$y = \frac{1}{\pi}\int \varphi \, d\theta$		
	0.2472	66.8000	1.0000	6.8000	0.5		
X/L	0.146	0.26	0.375	0.57	0.759	0.814	1
Tw_0	22.7000	23.6000	22.5000	22.6000	23.2000		
Tw_π	22.5000	21.3000	19.8000	18.9000	17.7000	14.7000	
T_B	8.29	9.56	10.89	13.22	15.53	16.21	18.53
α_0	27.27	27.99	33.84	41.89	51.23	-------	
α_π	27.65	33.47	44.10	69.18	181.1	-------	
$T\theta$	22.6000	22.5000	20.4000	19.3000	18.9000		
Re	.239+05	.220+05	.204+05	.181+05	.164+05	.159+05	
Pr	.767	.732	.715	.702	.700	.700	
Gr	.646+11	.272+11	.130+11	.459+10	.200+10	.161+10	
Gr_L	.257+08	.196+08	.154+08	.109+08	.827+07	.768+07	
Nu_R $\theta = \pi$	.317	.387	.512	.800	2.08	-------	
Nu_R $\theta = 0$	.313	.324	.393	.484	.589	-------	
Nu_R Avg.	.315	.356	.452	.642	1.34	-------	
ψ or ψ^* $\theta = 0$	3.43	2.85	2.26	1.79	1.53	-------	
ψ or ψ^* $\theta = \pi$	3.40	2.55	1.97	1.48	1.15	-------	
ψ or ψ^* Avg.	3.41	2.70	2.12	1.63	1.34	-------	

†Flow unstable, results questionable.

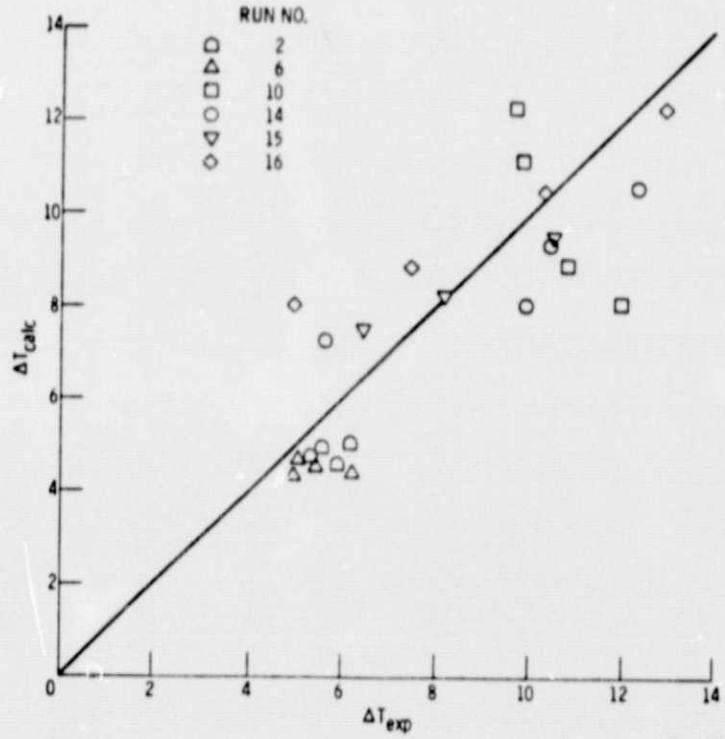

Figure A1. - Variation of calculated ΔT with experimental ΔT for $\bar{Nu}_R \sim \frac{4}{5} \bar{\Psi}^{-4/5}$.

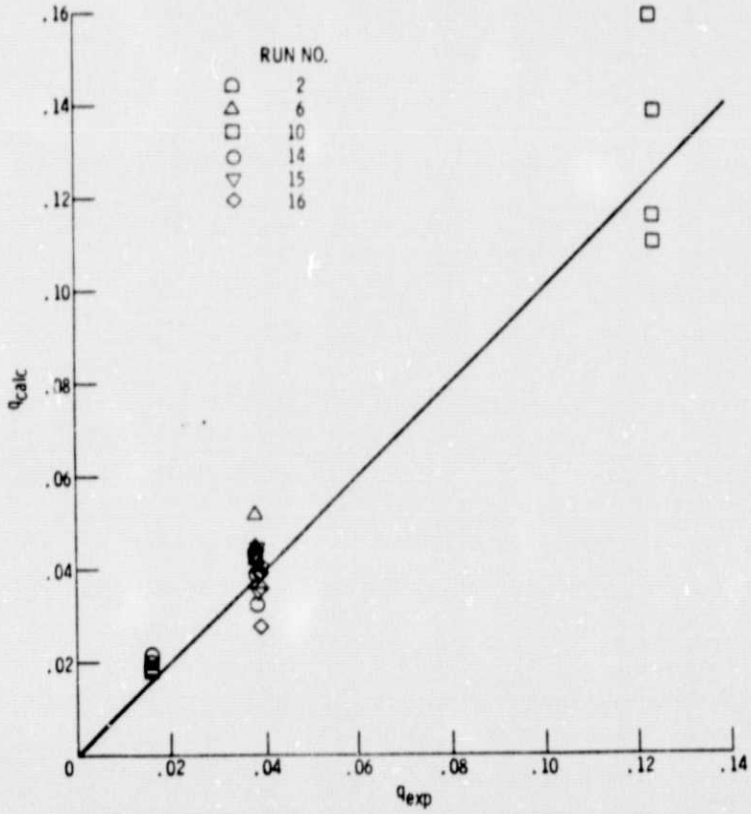

Figure A2. - Variation of calculated heat flux with experimental heat flux for $\bar{Nu}_R \sim \frac{4}{5} \bar{\Psi}^{-4/5}$.

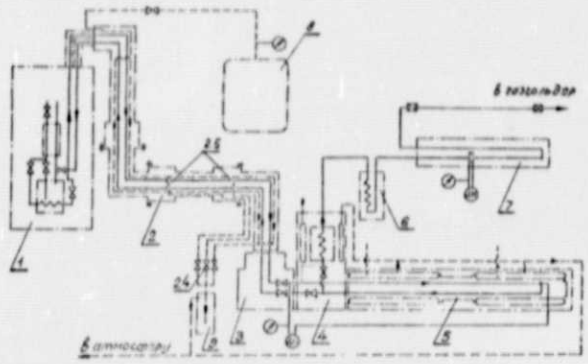

Рис. 3.1. Гидравлическая схема установки

Figure 1. - Schematic of the experimental apparatus.

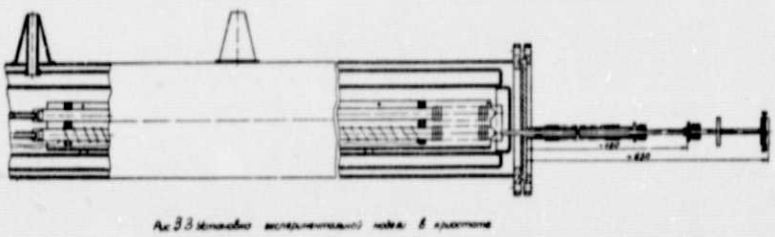

Figure 2. - Schematic of the test section.

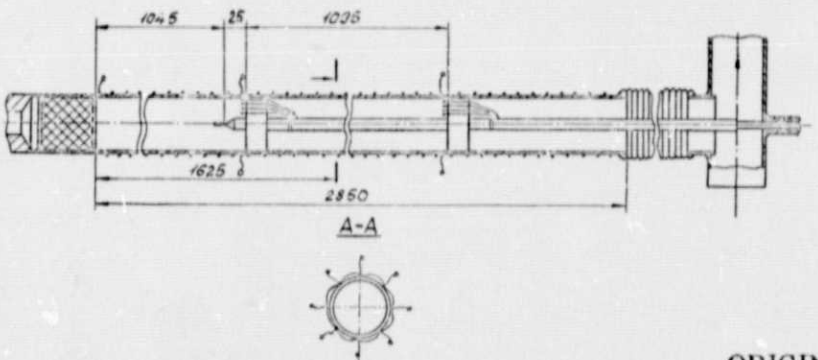

Рис. 3.4. Эскиз экспериментальной модели

Figure 3. - Internal probe and thermocouple locations.

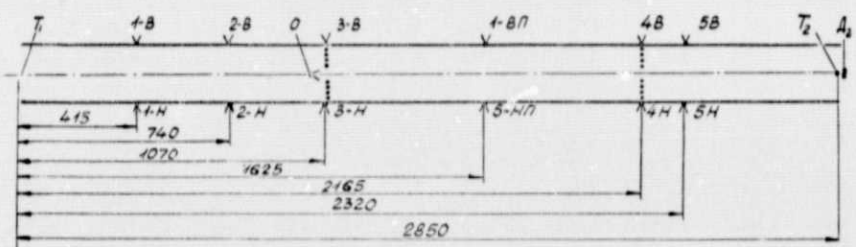

Рис. 3.6. Схема расположения термопар и датчиков на экспериментальном участке

Figure 4. - Schematic of test section thermocouple locations.

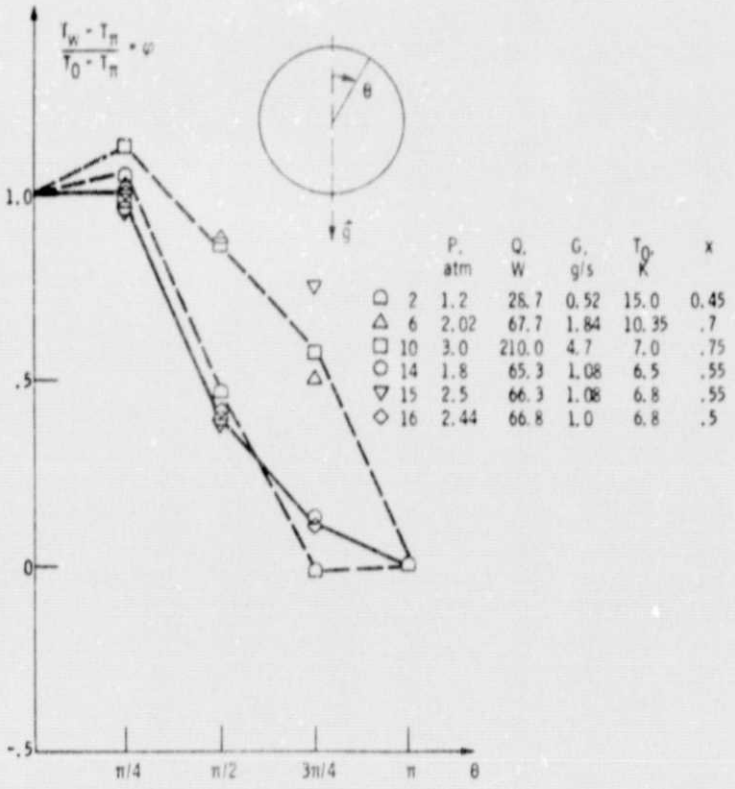

Figure 5. - Variation of wall reduced temperature with angular position for near critical helium flowing in a heated horizontal pipe.

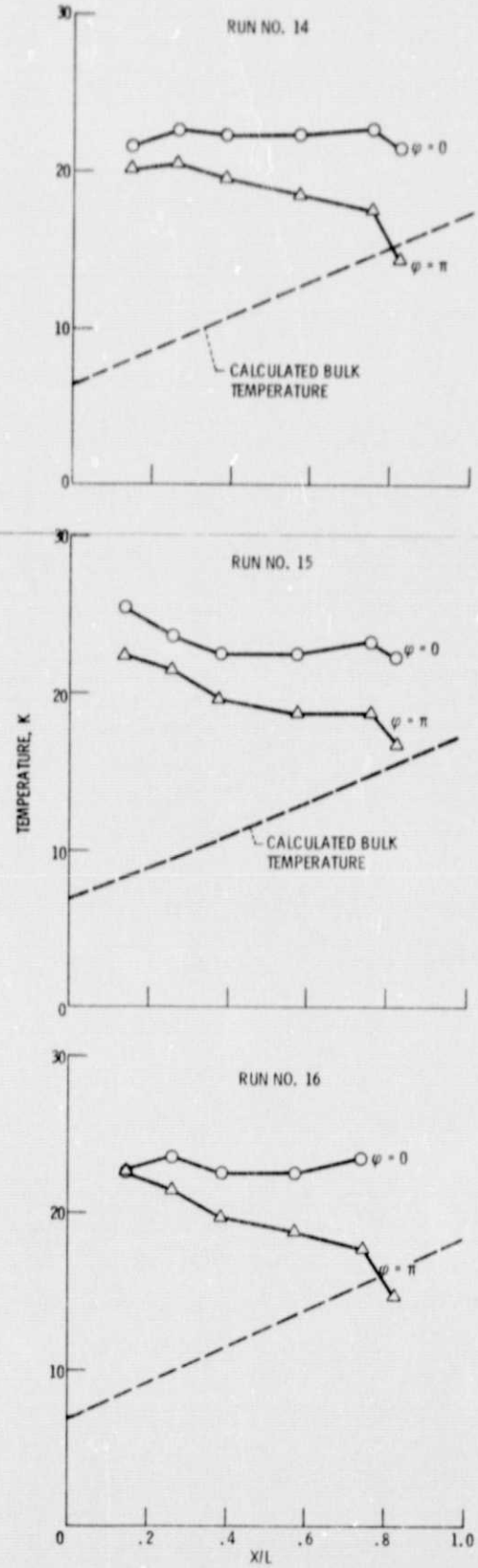

Figure 6. - Typical axial temperature profiles for fluid helium in a uniformly heated horizontal pipe.

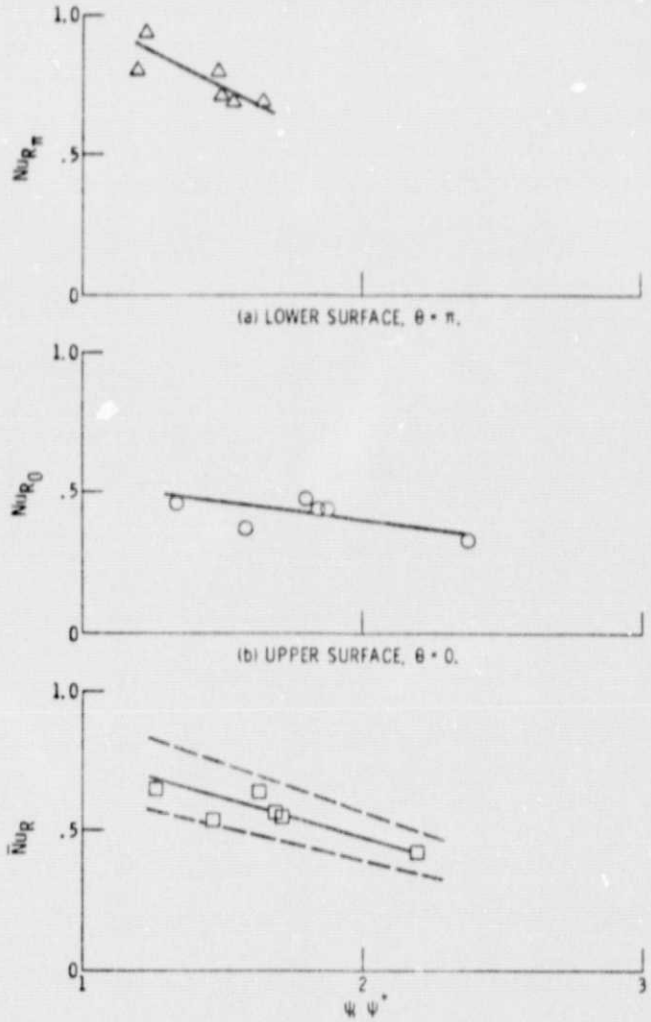

Figure 7. - Thermogravitational effects of near critical fluid helium flowing through a horizontal pipe with uniform heat flux at X/L = 0.57.

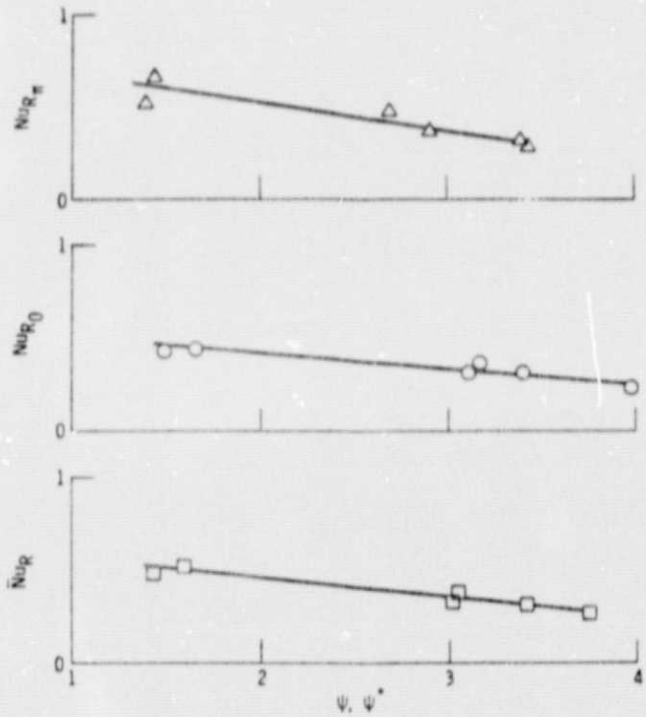

(a) X/L = 0.146.

Figure 8. - Thermogravitational data for helium flowing in a horizontal tube at the lower surface θ = π, upper surface θ = 0, and the average effect.

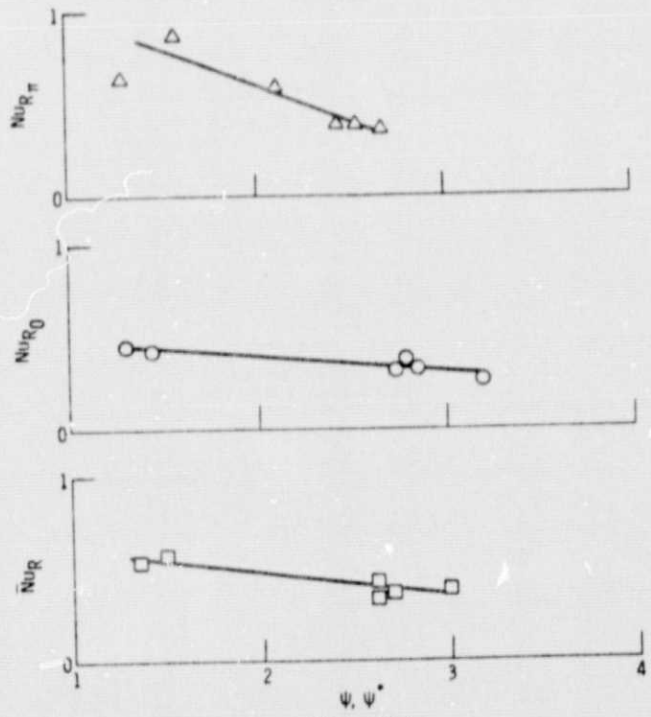

(b) X/L = 0.26.

Figure 8. - Continued.

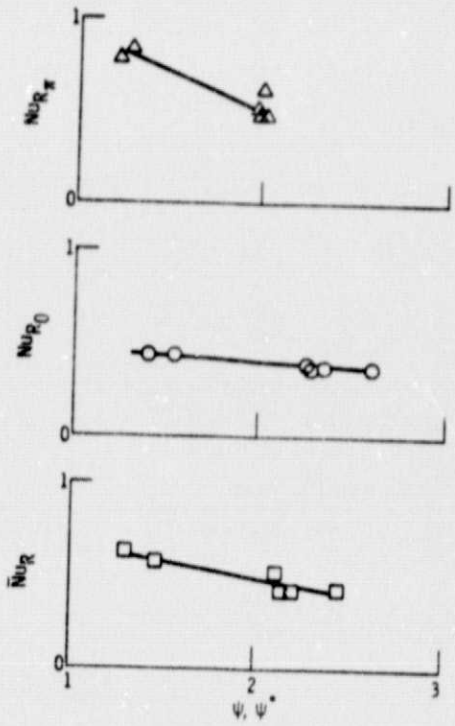

(c) X/L = 0.375.

Figure 8. - Continued.

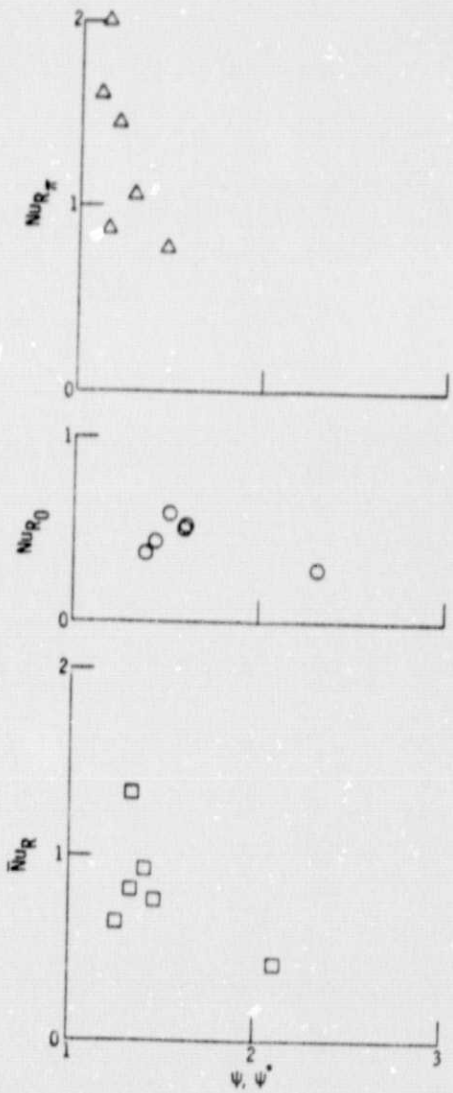

(d) X/L = 0.759.

Figure 8. - Concluded.

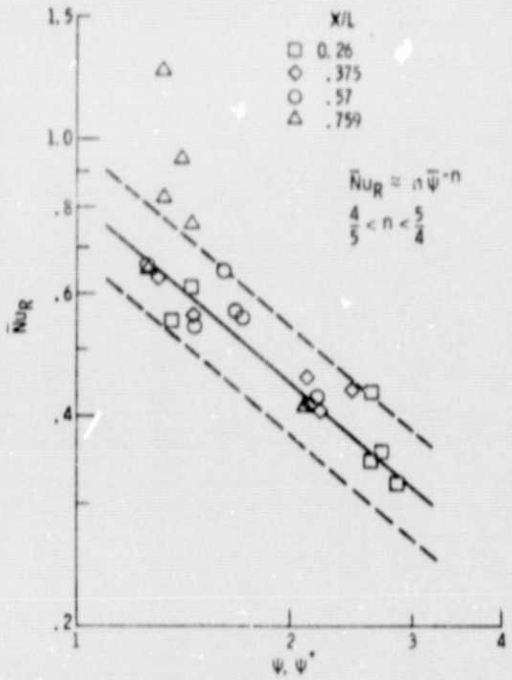

Figure 9. - Thermogravitational effects of near critical helium flowing horizontally through a uniformly heated pipe. Values averaged over the circumference based on X/L = 0.57.

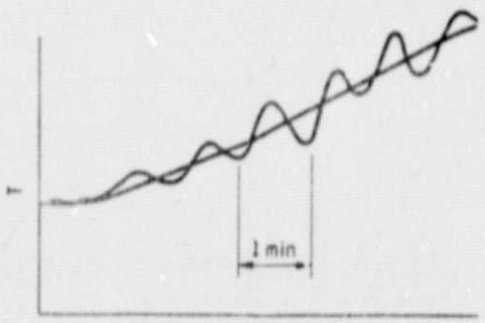

(a) GROWTH OF DISTURBANCE, τ.

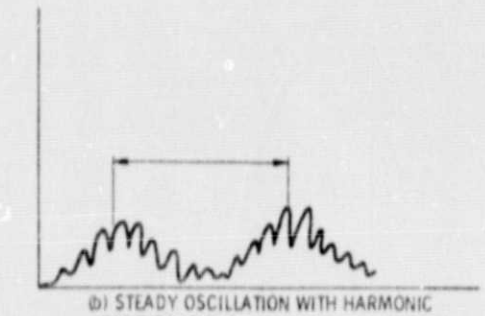

(b) STEADY OSCILLATION WITH HARMONIC PERTURBATIONS.

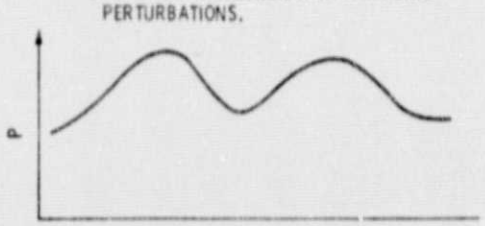

(c) INLET PRESSURE PERTURBATION, τ.

Figure 10. - System-refrigerator induced oscillations.

(a) Do/Di = 1.3.

Figure 11. - Mach Zender photograpgs of natural convection on air in confined cylinder. Courtesy: Prof. U. Grigill, Technical University of Munich, Munich, F.R.G.

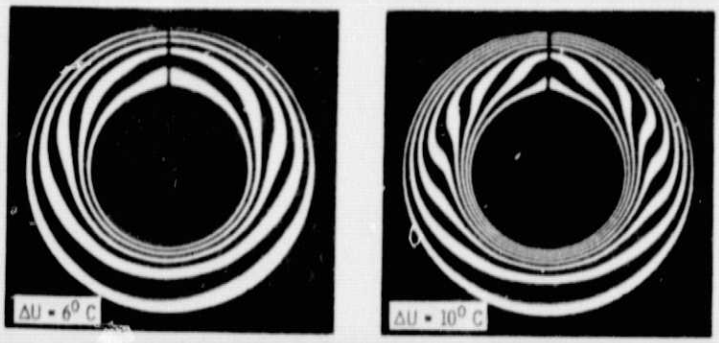

(b) Do/Di = 1.95.

Figure 11. - Continued.

(c) Do/Di = 3.9.

Figure 11. - Continued.

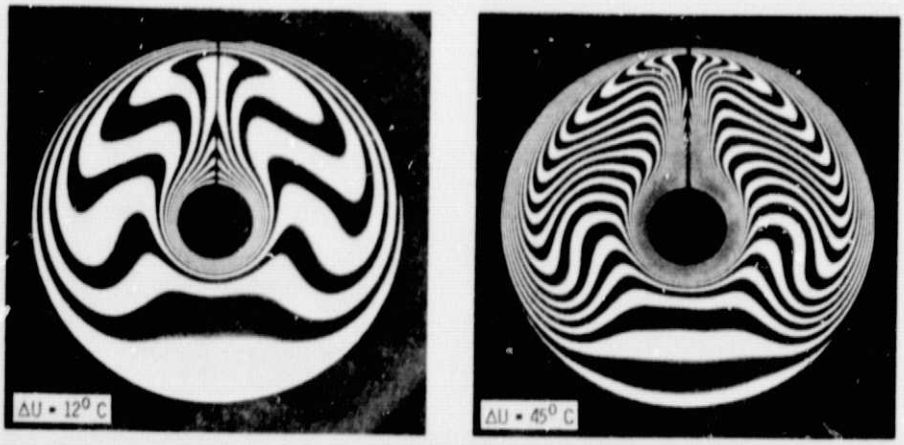

(d) Do/Di = 4.9.

Figure 11. - Concluded.